Photoelectron Angular Distributions for Two-photon Ionization of Helium by Ultrashort Extreme Ultraviolet Free Electron Laser Pulses

R Ma[1,2,3], K Motomura[1,2], K L Ishikawa[4], S Mondal[1], H Fukuzawa[1,2], A Yamada[1,2], K Ueda[1,2], K Nagaya[2,5], S Yase[2,5], Y Mizoguchi[2,5], M Yao[2,5], A Rouzée[6,7], A Hundermark[6,7], M J J Vrakking[6,7], P Johnsson[8], M Nagasono[2], K Tono[9], T Togashi[9], Y Senba[9], H Ohashi[2,9], M Yabashi[2] and T Ishikawa[2]

[1]Institute of Multidisciplinary Research for Advanced Materials, Tohoku University, Sendai 980-8577, Japan
[2]RIKEN SPring-8 Center, Hyogo 679-5148, Japan
[3]Institute of Atomic and Molecular Physics, Jilin University, Changchun 130012, China
[4]Photon Science Center, Graduate School of Engineering, The University of Tokyo, 7-3-1 Hongo, Bunkyo-ku, Tokyo 113-8656, Japan
[5]Department of Physics, Kyoto University, Kyoto 606-8502, Japan
[6]Max-Born-Institut, Max-Born Strasse 2A, D-12489 Berlin, Germany
[7]FOM Institute AMOLF, Science park 102, 1098 XG Amsterdam, Netherlands
[8]Department of Physics, Lund University, 22100 Lund, Sweden
[9]Japan Synchrotron Radiation Research Institute, Sayo, Hyogo 679-5198, Japan

E-mail: ueda@tagen.tohoku.ac.jp

E-mail: ishiken@atto.t.u-tokyo.ac.jp

Abstract. Two-photon ionization of helium atoms by ultrashort extreme-ultraviolet free-electron laser pulses, produced by the SPring-8 Compact SASE Source test accelerator, was investigated at photon energies of 20.3, 21.3, 23.0, and 24.3 eV. The angular distribution of photoelectrons generated by two-photon ionization is obtained using a velocity map imaging spectrometer. The phase-shift differences and amplitude ratios of the outgoing s and d continuum wave packets are extracted from the photoelectron angular distributions. The obtained values of the phase-shift differences are distinct from scattering phase-shift differences when the photon energy is tuned to a resonance with an excited level or Rydberg manifold. The difference stems from the co-presence of resonant and non-resonant path contributions in two-photon ionization by femtosecond pulses. Since the relative contribution of both paths can be controlled in principle by the pulse shape, the present results illustrate a new way to tailor the continuum wave packet.

PACS numbers: 32.80.Rm, 32.80.Fb, 41.60.Cr

1. Introduction

Two-photon processes are well-known phenomena and have been extensively investigated for decades both experimentally and theoretically. Also these processes have been used in a variety of applications in laser optics and spectroscopy. It is also well known that the angular distribution of photoelectrons generated by multi-photon processes is directly related to the relative amplitudes and the relative phase between different partial waves [1, 2, 3, 4, 5, 6]. However, these earlier works dealt with the laser pulses in the optical range whose pulse width is very long in comparison with the modern standard of femtosecond (fs) laser technology.

The advent of near infrared (IR) fs lasers opened new opportunity to investigate angular distributions of resonant enhanced multi-photon ionization (REMPI) of low ionization energy samples such as alkaline metals; here one of the the main interests was coherent control of the REMPI processes by the very intense near IR chirped fs pulses [7, 8]. For another directions of investigations for photoelectron angular distributions explored by the fs lasers, such as the time-solved measurements, see, for example, a recent review article [9].

The advent of extreme-intense short-wavelegnth lasers, i.e. extreme ultraviolet (EUV) [10, 11] and x-ray [12, 13] free-electron lasers (FELs), with femtosecond pulse widths, has led to renewed interest in two-photon processes in the EUV to x-ray regimes (see, e.g., [14, 15, 16, 17, 18, 19, 20, 21, 22]). In the present paper we address a new opportunity opened by the ultrashort EUV FEL pulses to deviate the phase shift difference between ionization channels from the scattering phase shift difference, which is otherwise intrinsic to the target atom or molecule. This will eventually open a new avenue to the coherent control of the continuum wave packets by the EUV pulses.

The simplest possible two-photon process may be single-color two-photon single ionization of helium atoms. For theoretical study, see, for example, the work by Nikolopoulos *et al.* [23], van der Hart and Bingham [24], and references cited therein. Kobayashi *et al.* [25] were the first to observe this process and used it for an autocorrelation measurement of high-order harmonic pulses, and Moshammer *et al.* [26] recently used it for an autocorrelation measurement of the EUV FEL pulses provided by the SPring-8 Compact SASE Source (SCSS) test accelerator [11]. The absolute two-photon ionization cross sections of He were measured using an intense high harmonic source [27] as well as the SCSS test accelerator [28]. Hishikawa *et al.* [29] recently investigated two- and three-photon ionization of He at the SCSS test accelerator by photoelectron spectroscopy using a magnetic bottle spectrometer. The photoelectron angular distribution (PAD) for single-color two-photon ionization of helium, however, has not been investigated so far, except in the context of multi-color above-threshold ionization [30, 31].

Two-photon single ionization of helium produces a continuum electron wave packet which is a superposition of s ($1s\,\epsilon s\ ^1S$) and d ($1s\,\epsilon d\ ^1D$) partial waves. For the wavelength range considered in this study ($51-61$ nm), the electric dipole approximation

is valid, and there is no two-photon excitation to auto-ionizing resonances. The PAD provides information about the ratio of amplitudes for the s and d partial waves and their relative phase. Haber *et al.* [32] have recently measured the PAD from near IR- and UV-laser-induced (single-photon) ionization of the $1snp$ excited states, which are prepared using high-order harmonics. A similar experiment has also been performed by O'Keeffe *et al.* [33] using synchrotron radiation for the preparation of excited states and a laboratory laser for the ionization. Both these experiments have confirmed that the relative phase between the s and d waves extracted from the measured PADs agrees well with the values expected from the theoretically calculated scattering phase shifts. In these studies the results were dominated by the dynamics of a resonant intermediate state. In the present work, in contrast, we investigate the situation in which resonant and non-resonant pathways coexist with similar probabilities, namely, (single-color) two-photon ionization by a femtosecond pulse. As theoretically predicted by Ishikawa and Ueda [34], this causes changes to the relative phase between the s and d waves which depend on wavelength. When the central wavelength is tuned to the resonance with an excited level, and for the case of fs pulses, both contributions from resonant and non-resonant ionization paths are significant, which leads to a relative phase between s and d that is distinct from the corresponding scattering phase difference. It is expected that this change in the phase difference can be revealed by means of a PAD measurement. The contribution of the non-resonant portion becomes negligible for longer pulses and for the two-step schemes as mentioned above [32, 33].

In the present study, we use the velocity map imaging (VMI) technique [35, 36] to measure the PAD from single-color two-photon ionization of He by femtosecond EUV FEL pulses. The anisotropy parameters are obtained from the PAD to extract the phase differences δ and the amplitude ratios of the s and d partial waves. Our results show the presence of an extra phase shift due to comparable contributions from resonant and non-resonant paths, in agreement with our recent theoretical prediction [34] and simulation results obtained by solving the full time-dependent Schrödinger equation.

2. Experiment

The experiments were carried out with the SCSS test accelerator in Japan. This FEL light source provided EUV pulses with a duration of ~ 30 fs [26] and a full-width-at-half-maximum spectral width of ~ 0.2 eV [37]. The present experiment was designed in a following manner. The photon energies were selected to be 20.3, 21.3, 23.0, and 24.3 eV. A photon energy of 20.3 eV is well below the excitation energy to the lowest resonance $1s2p\,^1P$ (21.218 eV) [38] and, thus, ionization is expected to be dominated by direct, non-resonant two-photon ionization. Conversely, the $1s2p\,^1P$ and $1s3p\,^1P$ (23.087 eV) [38] states can be resonantly excited at 21.3 and 23.0 eV due to the bandwidth of the FEL pulse, and according to our recent theoretical predictions [34], we may expect that both resonant and non-resonant contributions are involved in the photoionization process. A photon energy of 24.3 eV corresponds to excitation to the $1snp\,^1P$ Rydberg manifold

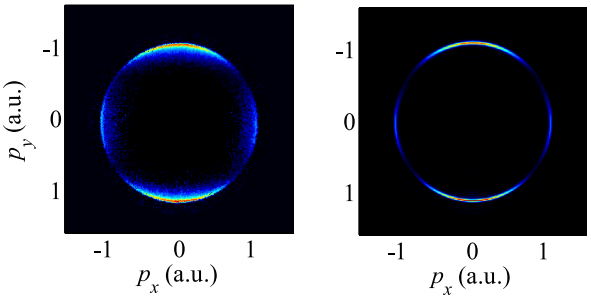

Figure 1. 2D projection (left) of the momentum distribution of the outgoing photoelectrons from two-photon ionization of helium atoms at 20.3 eV photon energy, and corresponding slice (right) through the retrieved 3D photoelectron momentum distribution obtained from an Abel inversion.

($n \sim 7$). The spectral width covers several Rydberg members from $1s6p\ ^1P$ to $1s9p\ ^1P$. In this condition we also expect that resonant and non-resonant path contributions are co-present. Doubly excited states are not accessible through two-photon transitions by the photon energy range used in this study.

The FEL beam from the SCSS test accelerator was steered by two upstream plane SiC mirrors, passed a gas monitor detector (GMD), and then entered the prefocusing system of the beam line. The GMD was calibrated using a cryogenic radiometer [39]. The average pulse energy measured by the GMD during the experiments was $7-11$ μJ, with a standard deviation of $2-4$ μJ. The focusing system, with a focal length of 1 m, consisted of a pair of elliptical and cylindrical mirrors coated with SiC [40]. The reflectivity of each mirror was 70 %. Before entering the interaction chamber, the FEL beam passed through two sets of light baffles, each consisting of three skimmers with 4.0 mm and 3.5 mm diameters, respectively. These baffles successfully removed the majority of the scattered light specularly and non-specularly reflected by the two mirrors, without reducing the photon flux. The FEL beam was then focused on a helium beam at the center of a VMI spectrometer [41]. The measured focal spot size was ~ 13 μm in radius, resulting in an average intensity of typically $2-3\times10^{13}$ W/cm^2.

Electrons produced by two-photon ionization of the helium atoms by the FEL pulses were accelerated, perpendicularly to both the propagation and linear polarization axes of the FEL beam, towards a position-sensitive detector consisting of a set of microchannel plates (MCPs) followed by a phosphor screen. The positions of detected electrons were recorded using a gated CCD camera synchronized to the arrival of the FEL pulse in the interaction chamber. A 200 ns electrical gate pulse was applied to the back of the MCPs. In our measurements, the photoelectron angular distribution (PAD) has cylindrical symmetry along the FEL polarization, and we can retrieve the three-dimensional (3D) photoelectron momentum distribution from the measured 2D projection of the momentum distribution using a mathematical procedure based on an Abel inversion, where we express the photoelectron angular distribution in terms of a Legendre expansion. Examples of raw and inverted images are given in Fig. 1.

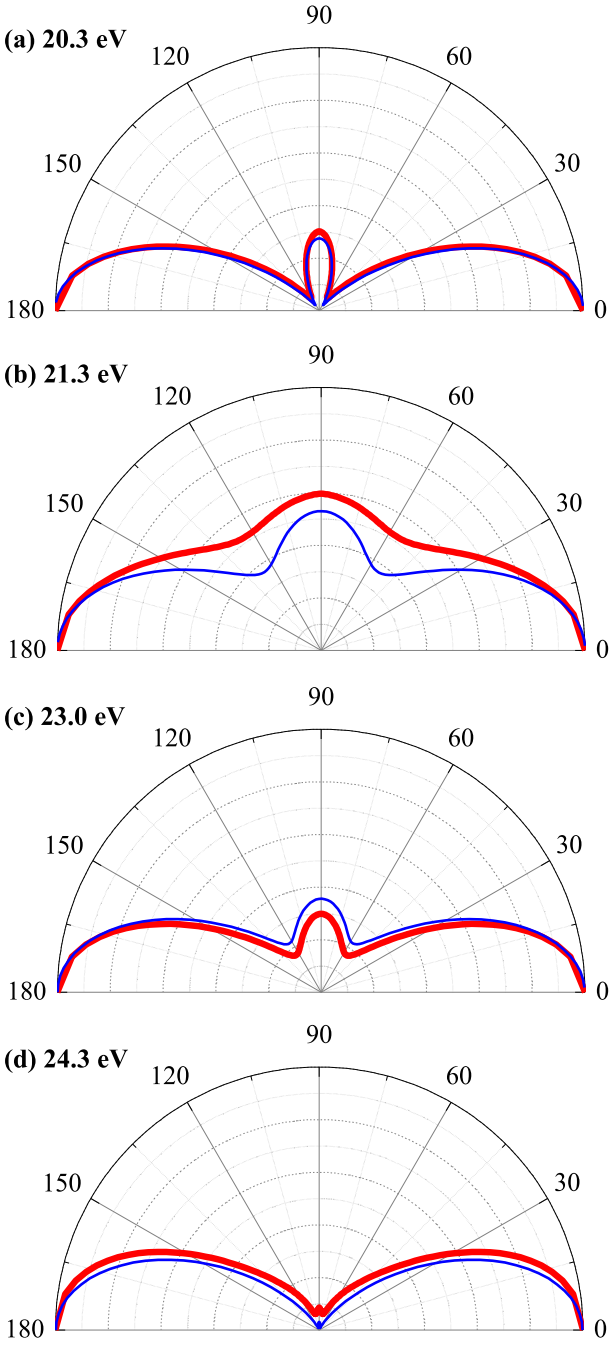

Figure 2. Measured (thick red lines) and calculated (thin blue lines) photoelectron angular distributions for two-photon ionization of helium. The experimental PADs are constructed from the β_l values extracted from the Abel inversion procedure.

3. Results and discussion

Figure 2 displays the PADs $I(\cos\theta)$ obtained at four different photon energies, as a function of cosine of the polar angle θ relative to the polarization axis. The PADs

Table 1. Experimentally obtained anisotropy parameters β_2 and β_4, and the extracted values of W and Δ.

$\hbar\omega$ (eV)	β_2	β_4	W	Δ
20.3	1.14±0.07	1.96±0.03	0.561±0.016	1.60±0.05
21.3	0.268±0.019	0.384±0.063	2.39±0.23	1.61±0.04
23.0	0.948±0.010	1.32±0.15	0.977±0.116	1.67±0.04
24.3	2.11±0.10	0.841±0.006	1.43±0.01	2.47±0.07

$I(\cos\theta)$ can be described by the following expression:

$$I(\cos\theta) = \frac{I_0}{4\pi}\left[1 + \beta_2 P_2(\cos\theta) + \beta_4 P_4(\cos\theta)\right] , \tag{1}$$

where I_0 is the angle-integrated intensity, β_2 and β_4 are the anisotropy parameters associated with the second- and fourth-order Legendre polynomials $P_2(x)$ and $P_4(x)$, respectively. Values of β_2 and β_4 obtained from the experimental PADs are listed in Table 1.

To investigate the processes involved in the two photon ionization of He, we have performed numerical simulations, by solving the full-dimensional two-electron time-dependent Schrödinger equation (TDSE) using the time-dependent close-coupling method [42, 43, 44, 45, 46]. We have employed chaotic pulses with a mean intensity of $2.5 \times 10^{13}\,\mathrm{W/cm^2}$, generated by the partial-coherence method described in Ref. [47], for a coherence time of 8 fs and a mean pulse width of 28 fs (full width at half maximum), as recently measured by second-order autocorrelation [26], both assumed to have Gaussian profiles on average. The effect of the slight difference of the actual pulse profiles from Gaussian is small compared with that of the difference between coherent and chaotic pulses as well as that of shot-to-shot fluctuation. One can see a good agreement between the experimental and simulation results in Fig. 2 as well as in Fig. 3 below.

The PAD results from an interference of the s and d partial waves, and can be expressed as,

$$\propto \left|c_0 e^{i\delta_{sc,0}} Y_{00} - c_2 e^{i\delta_{sc,2}} Y_{20}\right|^2 = \left||c_0| e^{i\delta_0} Y_{00} - |c_2| e^{i\delta_2} Y_{20}\right|^2 , \tag{2}$$

where c_l denotes the complex amplitude of a final state with an angular momentum l, $\delta_{sc,l}$ the scattering phase shift intrinsic to the corresponding continuum eigen function, and $\delta_l = \arg c_l + \delta_{sc,l}$ the phase of each partial wave. If we note that $Y_{l0}(\theta) = \sqrt{\frac{2l+1}{4\pi}} P_l(\cos\theta)$ and define $W = |c_0/c_2|$ and $\Delta = \delta_0 - \delta_2$, then, these are related to the anisotropy parameters as,

$$\beta_2 = \frac{10}{W^2+1}\left[\frac{1}{7} - \frac{W}{\sqrt{5}}\cos\Delta\right], \quad \beta_4 = \frac{18}{7(W^2+1)}, \tag{3}$$

and thus W and Δ can be extracted from the PAD. The experimentally obtained values of W and Δ are listed in Table I. Furthermore, in Fig. 3, the experimental values of W and Δ are compared with values extracted from TDSE simulations as described in [48], as a function of photon energy $\hbar\omega$. The agreement between experimental and theoretical

values are reasonable for both W [panel (a)] and Δ [panel (b)]. For comparison, theoretical values of the scattering phase shift difference $\Delta_{sc} \equiv \delta_{sc,0} - \delta_{sc,2}$ [49] are also plotted by the solid line.

Within the framework of the second-order time-dependent perturbation theory [34], c_l can be defined in such a way that its real and imaginary parts correspond to the resonant and non-resonant paths, respectively. If the pulse is non-resonant, c_0 and c_2 are pure imaginary, resulting in $\Delta = \Delta_{sc}$. In the present study, the measurement at $\hbar\omega = 20.3\,\mathrm{eV}$ corresponds to this situation; indeed, we find $\Delta \approx \Delta_{sc}$ in this case in Fig. 3.

Let us now turn to the situation where the pulse is resonant with an excited state or Rydberg manifold. If a resonant two-photon ionization path is dominant, Δ is again close to Δ_{sc}, since c_0 and c_2 are both real. On the other hand, if the contributions from both the resonant (via a single or several resonant levels) and non-resonant paths (via all the intermediate levels) are present, then $\Delta \neq \Delta_{sc}$ in general [34] and an extra phase shift difference $\Delta_{ex} \equiv \Delta - \Delta_{sc} = \arg c_0/c_2$ occurs. In the present study, the pulses with $\hbar\omega = 21.3, 23.0$, and 24.3 eV induce resonant two-photon ionization via $1s2p\,^1P$, $1s3p\,^1P$, and a Rydberg manifold ($1snp\,^1P$ with $n = 6 - 9$), respectively. We can see in Fig. 3 that the relative phase Δ deviates from the scattering phase shift difference Δ_{sc} for these three photon energies; the difference Δ_{ex} increases gradually with increasing photon energy and becomes very significant at 24.3 eV. At $\hbar\omega = 21.3$ and 23.0 eV, the simulation values of Δ_{ex} are slightly smaller than for lower intensity, indicating the departure from the perturbative limit due to the high intensity. The observed deviation Δ_{ex} clearly demonstrates the co-presence of the resonant and non-resonant path contributions in the present experiments, as recently predicted in Ref. [34]. This situation presents a contrast to the case of the photoionization from excited p states [32, 33], where the non-resonant path is absent and, as a result, $\Delta = \Delta_{sc}$. Although the co-presence of the resonant and non-resonant path contributions has been implicitly used in coherent control of resonance-enhanced multi-photon processes (see, e.g., [7, 8, 52]), explicit consideration of intermediate levels other than the resonant one is not necessary in most cases. In the present study, on the other hand, the contribution from non-resonant intermediate levels is essential to account for Δ_{ex} [34], which explains why Δ_{ex} is larger for a higher photon energy, i.e., for smaller level spacing.

It may be worth pointing out the similarity between two-photon ionization via a Rydberg manifold and two-photon above-threshold ionization. In the case of the 24.3 eV excitation, the intense ultrashort EUV pulses used in the present study coherently excite several Rydberg states $1snp\,^1P$ with $n = 6 - 9$. When the spectral width of the pulse contains a sufficient number of Rydberg levels [50], the Rydberg manifold behaves similarly to the continuum near the threshold and both the relative phase Δ [34] and the TPI yield [51] would smoothly vary when measured by increasing the photon energy across the ionization threshold. It should be noted that the extra phase shift difference due to free-free transitions plays a significant role in recently observed time delays in photoemission by attosecond EUV pulses [53, 54, 55, 56, 57].

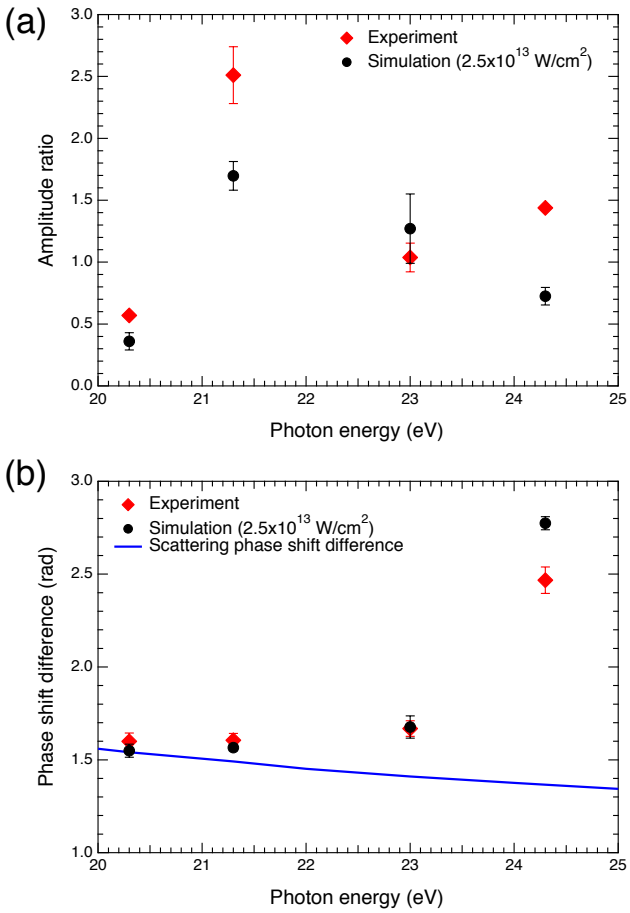

Figure 3. (a) Amplitude ratio W and (b) phase shift difference (relative phase) Δ extracted from experimental PADs (red diamonds) and calculated from wave functions obtained by TDSE simulations (black bullets). Theoretical scattering phase shift difference Δ_{sc} [49] is represented by a blue solid line in panel (b).

4. Conclusion

We have measured the PAD from two-photon ionization of He by femtosecond EUV FEL pulses provided by the SCSS test accelerator in Japan using a VMI spectrometer. From the anisotropy parameters of the PAD, we extracted phase-shift differences Δ and amplitude ratios W of the s and d partial waves at four different photon energies ($\hbar\omega = 20.3, 21.3, 23.0$, and 24.3 eV). As a result, we have demonstrated that the co-presence of the resonant and non-resonant path contributions in two-photon ionization by femtosecond pulses causes an additional phase shift in the photoelectron wavepacket. The relative contributions from the resonant and non-resonant paths can in principle be controlled by chirping the EUV pulses, which may pave a way to tailor continuum wave packets. Such an experiment will become feasible in the near future at FEL facilities where the pulses can be controlled in the range of a few to a few tens of fs.

Acknowledgments

We are grateful to the SCSS Test Accelerator Operation Group at RIKEN for continuous support in the course of the studies and to the staff of the technical service section in IMRAM, Tohoku University, for their assistance in constructing the apparatus. This study was supported by the X-ray Free Electron Laser Utilization Research Project of the Ministry of Education, Culture, Sports, Science and Technology of Japan (MEXT), by the Management Expenses Grants for National Universities Corporations from MEXT, by Grants-in-Aid for Scientific Research from JSPS (No. 21244062 and No. 22740264), and IMRAM research program. K.L.I. gratefully acknowledges support by the APSA Project (Japan), KAKENHI (No. 23656043 and No. 23104708), the Project of Knowledge Innovation Program (PKIP) of Chinese Academy of Sciences (Project No. KJCX2.YW.W10), and the Cooperative Research Program of Network Joint Research Center for Materials and Devices. The research of A.H., A.R. and M.V. is part of the research program of the "Stichting voor Fundamenteel Onderzoek der Materie (FOM)", which is financially supported by the "Nederlandse organisatie voor Wetenschappelijk Onderzoek (NWO)". P.J. acknowledges support from the Swedish Research Council and the Swedish Foundation for Strategic Research.

References

[1] S.N. Dixit and P. Lambropoulos, Phys. Rev. A **27**, 861 (1983).
[2] S.J. Smith and G. Leuchs, Adv. At. Mol. Phys. **24**, 157-221 (1988).
[3] P. Lambropoulos, P. Maragikis, and J. Zhang, Phys. Rep. **305**, 203 (1998).
[4] Z.-M. Wang and D.S. Elliott, Phys. Rev. Lett. **87**, 173001 (2001).
[5] K.L. Reid, Annu. Rev. Chem. **54**, 397 (2003).
[6] N.M. Kabachnik, S. Fritzsche, A.N. Grum-Grzhimailo, M. Meyer, and K. Ueda, Phys. Rep. **451**, 155 (2007).
[7] M. Krug, T. Bayer, M. Wollenhaupt, C. Sarpe-Tudoran, T. Baumert, S.S. Ivanov, and N.V. Vitanov, New J. Phys. **11**, 105051 (2009).
[8] M. Wollenhapt M. Klug, J. Köhler, T. Bayer, C. Sarpe-Tudoran, and T. Baumert, Appl. Phys. B **95**, 245 (2009).
[9] K.L. Reid, Mol. Phys. **110**, 131 (2012).
[10] W. Ackermann *et al.*, Nat. Photonics, **1**, 336 (2007).
[11] T. Shintake *et al.*, Nat. Photonics, **2**, 555 (2008).
[12] P. Emma *et al.*, Nat. Photonics, **4**, 641 (2010).
[13] T. Ishikawa *et al.*, Nat. Photonics **6**, 540 (2012).
[14] M. Nagasono *et al.*, Phys. Rev. A **75**, 051406 (2007).
[15] H. R. Varma, M. F. Ciappina, N. Rohringer, and R. Santra, Phys. Rev. A **80**, 053424 (2009).
[16] R. Santra, N. V. Kryzhevoi, and L. S. Cederbaum, Phys. Rev. Lett. **103**, 013002 (2009).
[17] L. Young *et al.*, Nature (London) **466**, 56 (2010).
[18] J..P. Cryan *et al.*, Phys. Rev. Lett. **105**, 083004 (2010).
[19] L. Fang *et al.*, Phys. Rev. Lett. **105**, 083005 (2010).
[20] N. Berrah *et al.*, Proc. Nat. Acad. Sci. **108**, 16912 (2011).
[21] G. Doumy *et al.*, Phys. Rev. Lett. **106**, 083002 (2011).
[22] P. Salén *et al.*, Phys. Rev. Lett. **108**, 153003 (2012).
[23] L.A.A. Nikolopoulos and P. Lambropoulos, J. Phys. B: At. Mol. Opt. Phys. **34**, 545 (2001).

[24] H.W. van der Hart and P. Bingham, J. Phys. B: At. Mol. Opt. Phys. **38**, 207 (2005).
[25] Y. Kobayashi, T. Sekikawa, Y. Nabekawa, and S. Watanabe, Opt. Lett. **23**, 64 (1998).
[26] R. Moshammer *et al.*, Opt. Express **19**, 21698 (2011).
[27] H. Hasegawa, E. J. Takahashi, Y. Nabekawa, K. L. Ishikawa, and K. Midorikawa, Phys. Rev. A **71**, 023407 (2005).
[28] T. Sato *et al.*, J. Phys. B: At. Mol. Opt. Phys. **44**, 161001 (2011).
[29] A. Hishikawa *et al.*, Phys. Rev. Lett. **107**, 243003 (2011).
[30] O. Guyétand, M. Gisselbrecht, A. Huetz, P. Agostini, R. Taïeb, V. Véniard, A. Maquet, L. Antonucci, O. Boyko, C. Valentin, and D. Douillet, J. Phys. B. **38**, L357 (2005).
[31] L. H. Haber, B. Doughty, and S. R. Leone, Phys. Rev. A **84**, 013416 (2011).
[32] L. H. Haber, B. Doughty, and S. R. Leone, Phys. Rev. A **79**, 031401(R) (2009).
[33] P. O'Keeffe, P. Bolognesi, R. Richter, A. Moise, E. Ovcharenko, L. Pravica, R. Sergo, L. Stebel, G. Cautero, and L. Avaldi, J. Phys.: Conf. Ser. **235**, 012006 (2010).
[34] K.L. Ishikawa and K. Ueda, Phys. Rev. Lett. **108**, 033003 (2012).
[35] A. T. J. B. Eppink and D. H. Parker, Rev. Sci. Instrum. **68**, 3477 (1997).
[36] A. Rouzee *et al.*, Phys. Rev. A **83**, 031401(R) (2011).
[37] Y. Hikosaka *et al.*, Phys. Rev. Lett. **105**, 133001 (2010).
[38] http://physics.nist.gov/PhysRefData/ASD/levels_form.html.
[39] M. Kato *et al.*, Nucl. Instrum. Methods Phys. Res. A **612**, 209 (2009).
[40] H. Ohashi *et al.*, Nucl. Instrum. Methods Phys. Res., Sect. A **649**, 58 (2011).
[41] E.V. Gryzlova *et al.*, Phys. Rev. A **84**, 063405 (2011).
[42] M. S. Pindzola and F. Robicheaux, Phys. Rev. A **57**, 318 (1998).
[43] M. S. Pindzola and F. Robicheaux, J. Phys. B **31**, L823 (1998).
[44] J. Colgan, M. S. Pindzola, and F. Robicheaux, J. Phys. B **34**, L457 (2001).
[45] J. S. Parker, L. R. Moore, K. J. Meharg, D. Dundas, and K. T. Taylor, J. Phys. B **34**, L69 (2001).
[46] K. L. Ishikawa and K. Midorikawa, Phys. Rev. A **72**, 013407 (2005).
[47] T. Pfeifer, Y. Jiang, S. Düsterer, R. Moshammer, and J. Ullrich, Opt. Lett. **35**, 3441 (2010).
[48] Ishikawa, K L and Ueda, K 2013 Photoelectron angular distribution and phase in two-photon single ionization of H and He by a femtosecond and attosecond extreme-ultraviolet pulse *Appl. Sci.* **3** 189-213
[49] T. T. Gien, J. Phys. B **35**, 4475 (2002).
[50] How dense the levels should be can be roughly estimated by investigating how well the integral $\int_{-\infty}^{\infty} e^{-x^2} dx$ can be approximated by the sum of the values at discrete points. One finds by simple calculations that the approximation is surprisingly good (within a 1% error) even if the discrete points are separated by 1.3 [48], while the full width at half maximum of e^{-x^2} is $2\ln 2 (= 1.665\cdots)$. In the present case, the spectral width is ≈ 0.23 eV, while the level spacing is at most 0.1 eV for $n = 6 - 9$. Therefore, the Rydberg manifold behaves similarly to the continuum [48].
[51] K. L. Ishikawa, Y. Kawazura, and K. Ueda, J. Mod. Opt. **57**, 999 (2010).
[52] N. Dudovich, B. Dayan, S.M. Gallagher Faeder, and Y. Silberberg, Phys. Rev. Lett. **86**, 47 (2001).
[53] M. Schultze *et al.*, Science **328**, 1658 (2010).
[54] K. Klünder *et al.*, Phys. Rev. Lett. **106**, 143002 (2011).
[55] M. Swoboda, T. Fordell, K. Klünder, J.M. Dahlström, M. Miranda, C. Buth, K.J. Schafer, J. Mauritsson, A. L'Huillier, and M. Gisselbrecht, Phys. Rev. Lett. **104**, 103003 (2010).
[56] J.M. Dahlström, A. L'Huillier, and A. Maquet, J. Phys. B: At. Mol. Opt. Phys. **45**, 183001 (2012).
[57] Dahlström J M, Guénot D, Klünder K, Gisselbrecht M, Mauritsson J, L'Huillier A, Maquet A and Taïeb R 2013 *Chem. Phys.* **414** 53